

# CDKL5 deficiency disorder: progressive brain atrophy may be part of the syndrome

Nicola Specchio<sup>1,\*†</sup>, Marina Trivisano<sup>1,†</sup>, Matteo Lenge<sup>2</sup>, Alessandro Ferretti<sup>1</sup>, Davide Mei<sup>2</sup>, Elena Parrini<sup>2</sup>, Antonio Napolitano<sup>3</sup>, Camilla Rossi-Espagnet<sup>4</sup>, Giacomo Talenti<sup>5</sup>, Daniela Longo<sup>4</sup>, Jacopo Proietti<sup>6</sup>, Francesca Ragona<sup>7</sup>, Elena Freri<sup>7</sup>, Roberta Solazzi<sup>7</sup>, Tiziana Granata<sup>7</sup>, Francesca Darra<sup>6</sup>, Bernardo Dalla Bernardina<sup>6</sup>, Federico Vigeveno<sup>8</sup>, Renzo Guerrini<sup>2</sup>

<sup>1</sup>Clinical and Experimental Neurology, Bambino Gesù Children's Hospital IRCCS, Rome 00165, Italy,

<sup>2</sup>Neuroscience Department, Meyer Children's Hospital IRCCS, Florence, 50139, Italy,

<sup>3</sup>Medical Physics Unit, Enterprise Risk Management, Bambino Gesù Children's Hospital, IRCCS, Rome 00165, Italy,

<sup>4</sup>Functional and Interventional Neuroimaging Unit, Bambino Gesù Children's Hospital, IRCCS, Rome 00165, Italy,

<sup>5</sup>Neuroradiology Unit, Azienda Ospedale-Università di Padova, Padova 35128, Italy,

<sup>6</sup>Child Neuropsychiatry Unit, Department of Surgical Sciences, Dentistry, Gynecology and Pediatrics, University of Verona, Verona 37121, Italy,

<sup>7</sup>Department of Pediatric Neuroscience, Fondazione IRCCS Istituto Neurologico Carlo Besta, Milano 20133, Italy,

<sup>8</sup>Research Area on Neurology and Neurorehabilitation, Bambino Gesù Children's Hospital IRCCS, Rome 00050, Italy

\*Corresponding author: Clinical and Experimental Neurology, Bambino Gesù Children's Hospital, IRCCS, Rome, P.zza S. Onofrio 4, 00165 Rome, Italy.

Email: nicola.specchio@opbg.net

†Nicola Specchio and Marina Trivisano contributed equally.

The clinical phenotype of Cyclin-Dependent Kinase-Like 5 (CDKL5) deficiency disorder (CDD) has been delineated but neuroimaging features have not been systematically analyzed. We studied brain magnetic resonance imaging (MRI) scans in a cohort of CDD patients and reviewed age at seizure onset, seizure semiology, head circumference. Thirty-five brain MRI from 22 unrelated patients were included. The median age at study entry was 13.4 years. In 14/22 patients (85.7%), MRI in the first year of life was unremarkable in all but two. In 11/22, we performed MRI after 24 months of age (range 2.5–23 years). In 8 out of 11 (72.7%), MRI showed supratentorial atrophy and in six cerebellar atrophy. Quantitative analysis detected volumetric reduction of the whole brain (−17.7%,  $P$ -value = 0.014), including both white matter (−25.7%,  $P$ -value = 0.005) and cortical gray matter (−9.1%,  $P$ -value = 0.098), with a reduction of surface area (−18.0%,  $P$ -value = 0.032), mainly involving the temporal regions, correlated with the head circumference ( $\rho$  = 0.79,  $P$ -value = 0.109). Both the qualitative structural assessment and the quantitative analysis detected brain volume reduction involving the gray and white matter. These neuroimaging findings may be related to either progressive changes due to CDD pathogenesis, or to the extreme severity of epilepsy, or both. Larger prospective studies are needed to clarify the bases for the structural changes we observed.

**Key words:** developmental and epileptic encephalopathy; brain atrophy; cerebellar atrophy; genetic epilepsy; CDD; CDKL5.

## Introduction

Cyclin-Dependent Kinase-Like 5 (CDKL5) deficiency disorder (CDD; OMIM 300203, 300672) is an X-linked developmental and epileptic encephalopathy (DEE) characterized by infantile-onset refractory epilepsy, hypotonia, severe developmental delay, and central visual impairment (Weaving et al. 2004; Bahi-Buisson et al. 2012; Olson et al. 2019; Zuberi et al. 2022). The CDKL5 protein is widely expressed in the brain, predominantly in neurons, with roles in neuronal proliferation, migration, axonal outgrowth, dendritic morphogenesis, and synapse development (Rusconi et al. 2008; Chen et al. 2010; Ricciardi et al. 2012; Zhu et al. 2013; Zhou et al. 2017; Zhu and Xiong 2019). CDD was initially identified as a variant of Rett syndrome; however, only 23.7% of patients meet clinical criteria for Rett syndrome and CDD-related severe and peculiar epilepsy phenotype have prompted its recognition as an independent phenotype (Guerrini and Parrini 2012; Olson et al. 2019).

Epilepsy is the earliest and predominant symptom, exhibiting peculiar electroclinical findings and evolutive characteristics

(Bahi-Buisson et al. 2008; Melani et al. 2011; Zuberi et al. 2022; Darra et al. 2023). Seizures are resistant to anti-seizure medications (ASMs) and, since most patients have daily seizures, both quality of life and neurodevelopment are severely impaired (Bahi-Buisson et al. 2008; Fehr et al. 2016; Demarest et al. 2019; Olson et al. 2019; Darra et al. 2023). Burden of the disease is further augmented by movement disorders, severe developmental delay, behavioral and sleep disturbances (Hagebeuk et al. 2013; Mangatt et al. 2016; Lo Martire et al. 2017; Arican et al. 2019; Kadam et al. 2019).

Neuroimaging has not been analyzed in CDD, except scattered case reports that have documented either normal brain anatomy or—less often—cortical atrophy or T2 fluid-attenuated inversion recovery hyperintensities in the white matter (Archer et al. 2006; Buoni et al. 2006; Bahi-Buisson et al. 2008; Bahi-Buisson et al. 2008; Elia et al. 2008; Pintaudi et al. 2008; Russo et al. 2009; Mei et al. 2010; Melani et al. 2011; Sartori et al. 2011; Olson and Poduri 2012; Stalpers et al. 2012; Olson et al. 2019; Tang et al. 2021). We report brain MRI features on a cohort of 22 patients with CDD studied across different ages.

Received: February 10, 2023. Revised: April 17, 2023. Accepted: June 19, 2023

© The Author(s) 2023. Published by Oxford University Press. All rights reserved. For permissions, please e-mail: journals.permissions@oup.com

This is an Open Access article distributed under the terms of the Creative Commons Attribution Non-Commercial License (<https://creativecommons.org/licenses/by-nc/4.0/>), which permits non-commercial re-use, distribution, and reproduction in any medium, provided the original work is properly cited. For commercial re-use, please contact journals.permissions@oup.com

## Materials and methods

All patients with CDD with available brain MRI images followed in four Italian pediatric epilepsy tertiary-care centers were enrolled. All four centers are part of the EpiCARE European Reference Network for Rare and Complex Epilepsies. All patients carried a pathogenic *CDKL5* genetic variant identified by different methods, including single gene Sanger sequencing, multiplex ligation-dependent probe amplification or next-generation sequencing (NGS) (Supplementary Table 1). We reviewed clinical data of all patients (age at seizure onset, seizure semiology presented at the latest observation, head circumference). We also performed a two-sample *t*-test analysis of the head circumference in patients versus age and sex matched healthy females.

Two pediatric neuroradiologists with at least 5 years' experience (C.R.E. and G.T.), and blinded to clinical data, retrospectively reviewed the MRI scans and, in case of discordant findings, reached a consensus agreement.

A common protocol was used to evaluate brain structures—deep and cortical gray matter, deep and peripheral white matter, commissures, midbrain, pons, medulla, cerebellar hemispheres, vermis, ventricles, and CSF spaces were considered. The criterion for atrophy was evidence of the widening of ventricles or subarachnoid spaces. Corpus callosum thinning was evaluated according to previously published biometric reference standards (Garel et al. 2011).

MRI scans were acquired on different magnets (1.5 or 3 T scanner) with non-standardized imaging protocols; however, all scans included at least a sagittal SE T1-weighted (TE: 10–15 ms, TR: 515–619 ms) or 3D MPRAGE (TE: 2.27 ms, TR: 2,060, IT: 1,040), axial TSE T2-weighted (TE: 100–122 ms, TR: 5,449–8,600 ms), coronal T2- (TE: 100–108 ms, TR: 4,300–6,380 ms) or Fluid-Attenuated Inversion Recovery (FLAIR), and axial FLAIR sequences (TE: 85–140 ms, TR: 9,000–11,000 ms, IT: 2,500 ms). All sequences had a slice thickness of 2–3 mm except the volumetric sequences with an isotropic voxel of 1 mm. The data that support the findings of this study are not openly available due to reasons of sensitivity and are available from the corresponding author upon reasonable request. Data are located in controlled access data storage at Bambino Gesù Children's Hospital in Rome.

## Quantitative MRI analysis

For a subset of five patients, we acquired high-quality T1-3D sequences, and quantitatively analyzed the volume, surface area, and thickness of the cortical mantle and volume of subcortical structures. We recruited 15 controls, three for each of the five patients, matched for sex and age. Controls had normal neurological examination and had performed a T1-3D MRI to investigate headache.

We assessed surface-based analysis of the cortical mantle adopting the FreeSurfer processing pipeline (version 7.1.1, <https://surfer.nmr.mgh.harvard.edu>). On both hemispheres, we performed cortical segmentation and 3D high-resolution reconstructions of the boundaries between white/gray and gray/cerebrospinal fluid. After the quality check of the 3D reconstructions by visual inspection and manual correction (where needed), we calculated the intra-cranial volume (ICV) and the thickness, surface area and volume of the whole cortical mantle.

We parceled the cortical surface of each hemisphere into 34 regions of interest (ROIs) using the Desikan et al. labeling system (Desikan et al. 2006) and calculated the averaged thickness, surface area and volume of each ROI.

We conducted statistical group analysis at whole-brain and ROI levels using FreeSurfer tools and MATLAB R2020a (Statistics and Machine Learning Toolbox Version 11.7, MathWorks Inc.).

At a whole-brain level, we smoothed cortical maps of morphometric (volume, area, and thickness) features (10 mm full width at half-maximum Gaussian kernel), clustered and corrected for multiple comparisons using the false discovery rate (FDR) with a cluster-wise correction approach (cluster-wise *P*-value < 0.05). To perform a vertex-wise analysis between the *CDKL5* and control groups, we adopted a linear regression model with the age and ICV as discrete covariates. We applied the same multivariable linear regression model to assess for each ROI between-group differences in volume, surface area and mean cortical thickness.

For subcortical analysis we used a QuickNAT neural network algorithm (<https://github.com/ai-med/QuickNATv2>) for automatic subcortical segmentation (Guha Roy et al. 2019). We segmented several areas (Gray and white matter, Putamen, Thalamus, Brainstem, Pallidum, Hippocampus, Amygdala, Caudate). We computed the volume for each subcortical area and scaled by the total intracranial volume as computed by the volume of GM and WM together. We included the mean value between left and right volumes of subcortical structures in the statistical analysis.

Statistical group analysis was conducted via MANOVA analysis on Putamen, Thalamus, Brainstem, Pallidum, Hippocampus, Amygdala, Caudate with the patient-control group as a fixed factor and age as a covariate of no interest. We then considered only significant results in the MANOVA for post hoc test with correction for multiple comparison via the Benjamini & Hochberg method. We also assessed the correlation between the head circumferences and estimated intra-cranial volumes.

## Results

We collected 35 brain MRI from 22 unrelated patients with CDD. The median age at study entry was 13.4 years (IQR 6.3–17.2 years). Most patients were female—16 (72.7%).

Table 1 and Fig. 1 summarize clinical and genetic data.

Supplementary Table 1 shows all the genetic variants in the study cohort. Head circumference of the *CDKL5*-mutated female patients was significantly lower, measured at a median age of 2.9 years (IQR 1.17–4.63) (*t*-value =  $-3.35$ ; *P*-value = 0.0013) if compared with controls (Supplementary Fig. 1).

In 14/22 patients, we performed brain MRI within the first year of life and considered it unremarkable for all (85.7%) but two patients, who had T2-hyperintensity in the central tegmental tracts. In 7 of 22 patients, we performed brain MRI between 12 and 24 months of age and observed mild supratentorial ventricular and CSF spaces enlargement with frontal predominance in six (85.7%) (Fig. 2A).

In 11/22 patients, we performed MRI after 24 months of age (range 2.5–23 years). In 8 out of 11 (72.7%), MRI showed supratentorial atrophy of variable severity, more prominent in the frontal lobes, at a median age of 5.5 years (IQR 2.4–11.8 years). In six of the previous eight patients, we detected cerebellar atrophy at a median age of 9.7 (IQR 4.3–12.9 years) (Fig. 2B–G).

Additional imaging findings were symmetric T2-hyperintensity involving the central tegmental tracts (in 4/22 patients, 18.2%), the posterior periventricular white matter (3/22 patients, 13.6%), and the dentate nuclei (3/22 patients, 13.6%) (Fig. 2H–M). Corpus callosum thinning was observed in 7/22 patients (31.8%).

Twelve patients had at least two MRIs. The median age at the second brain MRI was 30.5 months (IQR 15.5–40.75). Between the

**Table 1.** Clinical and genetic findings from the study cohort.

| Characteristic  | Value                 |                          |
|---|-----------------------|--------------------------|
| Patients, n   | 22                    |                          |
| <b>Sex, n (%)</b>   |                       |                          |
| Male  | 6 (27.3)              |                          |
| Female  | 16 (72.7)             |                          |
| <b>Age at study entry, median (IQR)</b>                     | 13.4 years (6.3–17.3) |                          |
| <b>Age at epilepsy onset, median (IQR)</b>                  | 8 weeks (3–12)        |                          |
| <b>Type of seizures, n (%)</b>                              |                       |                          |
| Tonic   | 18 (81.8)             |                          |
| Epileptic spasms  | 17 (77.3)             |                          |
| Myoclonic   | 7 (31.8)              |                          |
| Tonic-clonic  | 5 (22.7)              |                          |
| Clonic  | 4 (18.2)              |                          |
| Hyperkinetic  | 3 (13.6)              |                          |
| <b>Age at brain MRI, median (IQR)</b>                       |                       |                          |
| First   | 5 months (2–12)       |                          |
| Last  | 2.9 years (2.1–8.7)   |                          |
| <b>MRI findings (qualitative analysis)</b>                  | <b>Patients (n)</b>   | <b>Ages at brain MRI</b> |
| Mild supratentorial ventricular and CSF spaces              | 6/7                   | 12–24 m                  |
| Supratentorial atrophy                                      | 8/11                  | > 24 m                   |
| Cerebellar atrophy  | 2/11                  | > 24 m                   |
| T2-hyperintensity of central tegmental tracts               | 4/22                  | All ages                 |
| T2-hyperintensity of posterior periventricular white matter | 3/22                  | All ages                 |
| T2-hyperintensity of the dentate nuclei                     | 3/22                  | All ages                 |
| Corpus callosum thinning                                    | 7/22                  | all ages                 |

first and the last brain MRI, we detected the following changes: one patient developed supratentorial atrophy (time elapsed between the two brain MRIs: 1.58 years); six patients developed supratentorial and cerebellar atrophy (median time between the two brain MRIs: 4.6 years, IQR 1–10.5); one patient had a stable supratentorial and cerebellar atrophy (time elapsed between the two brain MRI: 1.42 years); two patients had stable supratentorial atrophy (median time between the two brain MRIs: 1.8 years, IQR 1.7–1.9); in two patients, no atrophic brain changes were present (median time elapsed between first and second MRI: 1.29 years, IQR 1.1–1.5).

Supplementary Fig. 2 shows the timing of MRI findings in relation with the three stages of epilepsy in patients with CDD. During the first stage (<10 weeks), the MRI was normal; in the second stage, supratentorial atrophy appeared in four patients; and in the third stage, cerebellar atrophy appeared in six patients.

### Quantitative MRI analysis

Using quantitative MRI analyses we uncovered volumetric reductions involving different brain structures. At a whole-brain level (Table 2), we observed a reduction in the total brain volume (–17.7%,  $P$ -value=0.014), the white matter (–25.7%,  $P$ -value=0.005), and the cortical gray-matter (–9.1%,  $P$ -value=0.098).

Volumetric reductions in the CDKL5 group were strongly associated with a decrease of the surface area (–18.0%,  $P$ -value=0.032), whereas the thickness of the cortical mantle was not significantly altered between CDKL5 and controls (+0.6%,  $P$ -value=0.895).

Cluster analysis (Table 3 and Fig. 3A) revealed significant volumetric reductions involving the temporal lobes bilaterally (the superior temporal gyrus with values:  $Z_{\max}$  = –4.02, area = 1,414.58 mm<sup>2</sup>, in the left hemisphere;  $Z_{\max}$  = –7.16, area = 853.37 mm<sup>2</sup>, in the right hemisphere; the left inferior

temporal gyrus, with  $Z_{\max}$  = –4.02, area = 411.30 mm<sup>2</sup>; the right middle temporal gyrus, with  $Z_{\max}$  = –4.38, area = 254.83 mm<sup>2</sup>), the anterior cingulate bilaterally, and the lingual gyri in the right hemisphere. We did not find significant clusters of altered surface area or cortical thickness.

At an ROI level (Table 3 and Supplementary Table 2), we observed a trend toward volumetric reduction in most lobes, bilaterally, mostly in the fronto-temporal regions (rostral middle frontal, pars opercularis, pars triangularis, pars orbitalis, medial orbitofrontal, rostral anterior cingulate, and superior, medial and inferior temporal). In these cortical regions, the volumetric reductions were associated with a significantly decreased area of the cortical surface. We did not observe alterations of cortical thickness.

Subcortical analysis revealed reduction of volume in three subcortical structures: hippocampus, amygdala, and thalamus (see the results in Table 2 and Fig. 3B).

We correlated the head circumference (cm) and the intracranial volume (cm<sup>3</sup>) and observed a strong, although not significant, correlation (coefficient  $\rho$  = 0.79,  $P$ -value = 0.109).

### Discussion

Although the clinical and genetic characterization of CDD has been intense, neuroimaging has not been systematically analyzed. Several case reports found normal brain anatomy and, rarely, white matter hyperintensity and cortical atrophy (Bahi-Buisson et al. 2008; Liang et al. 2011; Melani et al. 2011; Sartori et al. 2011).

At epilepsy onset, which is almost invariably within the second months of life, MRI has been reported to be either normal (Melani et al. 2011; Sartori et al. 2011) or show mild to moderate cerebral atrophy (Sartori et al. 2011). In our cohort, most patients

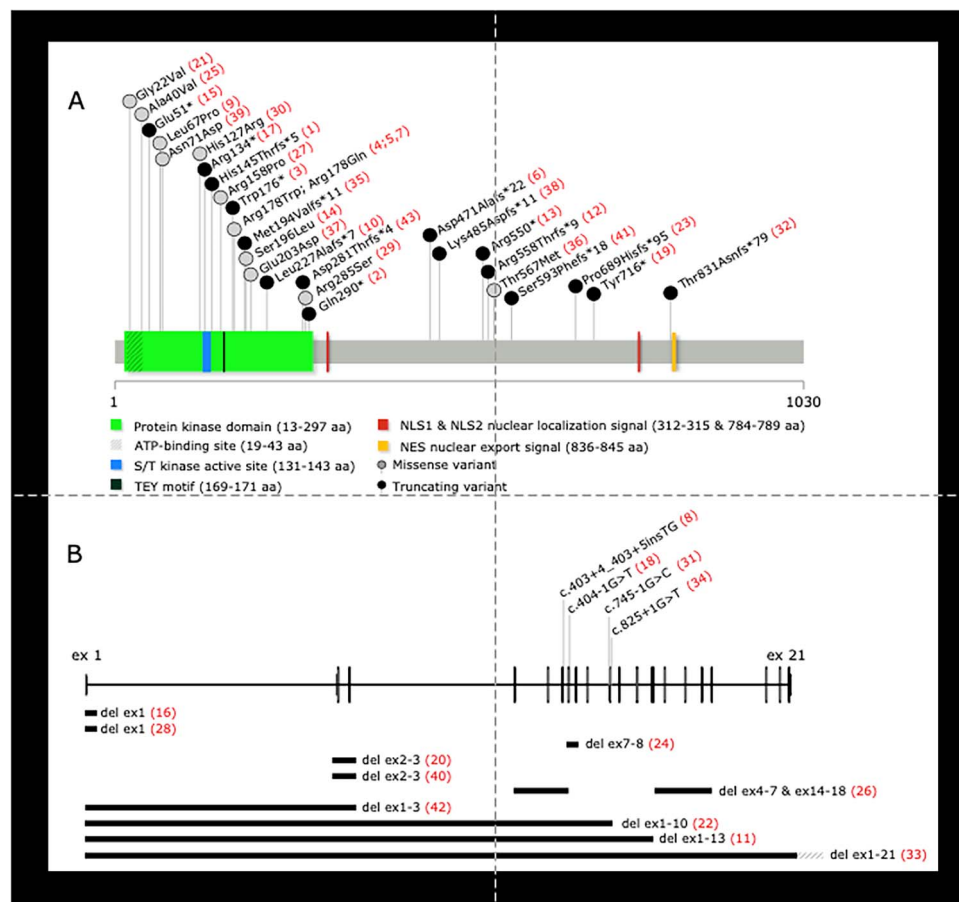


**Fig. 1.** Schematic representation of the CDKL5 protein (A) and genomic region (B). (A) The linear structure of the CDKL5 protein includes the protein kinase domain (light green), the ATP-binding site (dashed in the light green), the serine–threonine S/T kinase active site (blue), the threonine–Glutamate–tyrosine TEY phosphorylation motif (black), two nuclear localization signal 1 and 2 (red), and the nuclear export signal NES (ochre). The gray filled lollipops show the missense substitutions, whereas the black filled lollipops represent the stopgain and frameshift variants. Red numbers between round brackets correspond to the patients’ identifiers. aa: amino acid. (B) Schematic representation of the CDKL5 genomic region. The vertical black lines show the CDKL5 exonic regions. The 5’–3’ UTR (untranslated regions) and the coding regions are depicted with short and long vertical lines, respectively. Splicing variants and genomic rearrangements are reported above and below the CDKL5 genomic region, respectively. Gray dashed line indicates that the deletion is extended beyond the CDKL5 genomic region. Red numbers between round brackets correspond to the patients’ identifiers. ex: exon; del: deletion.

**Table 2.** Whole-brain analysis.

| Measurement              | CDKL5 group |            | Control group |            | t-value | P-value      | Difference between mean values (%) |
|--------------------------|-------------|------------|---------------|------------|---------|--------------|------------------------------------|
|                          | Mean value  | SD         | Mean value    | SD         |         |              |                                    |
| Total brain volume       | 811,098.40  | 221,416.83 | 985,153.60    | 118,374.56 | −2.753  | <b>0.014</b> | −17.7                              |
| Total cortical GM volume | 468,313.63  | 142,046.20 | 537,273.10    | 52,593.15  | −1.756  | 0.098        | −9.1                               |
| Total cerebral WM volume | 290,956.20  | 77,212.00  | 391,417.07    | 81,874.52  | −3.282  | <b>0.005</b> | −25.7                              |
| Hippocampus              | 0.0008      | 0.0002     | 0.0010        | 0.0002     |         | 0.06         | −20                                |
| Thalamus                 | 0.0046      | 0.0025     | 0.0060        | 0.0008     |         | <b>0.04</b>  | −23                                |
| Amygdala                 | 0.00030     | 0.00007    | 0.00040       | 0.00006    |         | <b>0.02</b>  | −25                                |
| Mean surface area        | 135,992.72  | 33,883.50  | 164,422.93    | 23,283.50  | −2.352  | <b>0.032</b> | −18.0                              |
| Mean cortical thickness  | 2.77        | 0.22       | 2.75          | 0.23       | −0.134  | 0.895        | 0.6                                |

Volume is expressed in mm<sup>3</sup>, surface area in mm<sup>2</sup>, and cortical thickness in mm; SD, standard deviation; GM, gray matter; WM, white matter; bold indicates statistical significance (P-value < 0.05) from linear regression models after controlling age (and intracranial volume for volume and area measurements).

(85.7%) had normal brain MRI at epilepsy onset, while the remaining had non-specific abnormalities such as T2-hyperintensity in the central tegmental tracts. From 12 to 24 months of age, enlarged mild supratentorial ventricular and CSF spaces with frontal predominance became apparent. After 3 years of age, supratentorial atrophy was easily identifiable and associated with cerebellar atrophy during the follow-up. Cerebral and cerebellar atrophy have previously been described in case series. Liang et al.

(Liang et al. 2011) reported cerebral atrophy predominant across bilateral frontal regions in 11 out of 12 patients with CDD and Bahi-Buisson et al. (Bahi-Buisson et al. 2008) mentioned cerebral atrophy in 13 patients with CDD (65%)—associated with mild cerebellar atrophy in two. Sartori et al., (Sartori et al. 2011) studied six patients and found mild to moderate cerebral atrophy in three within the first year of life, which was documented in one to have progressed after the age of 20 months. Fronto-temporal-insular

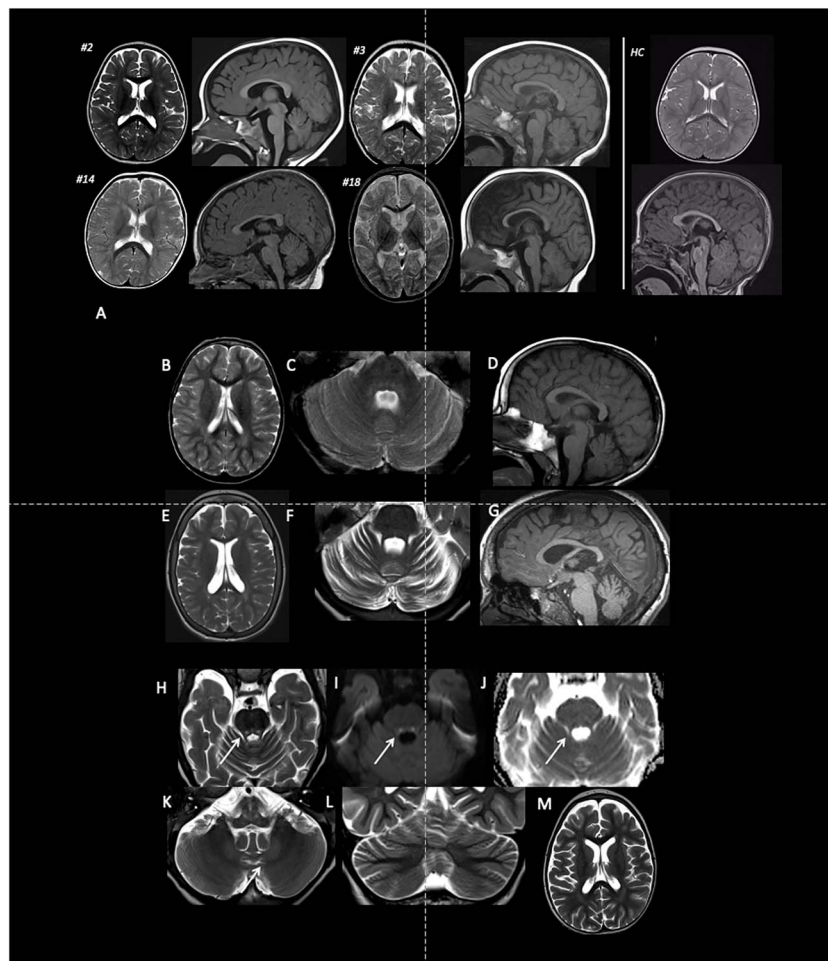


**Fig. 2.** MRI findings in CDD population of studied patients. (A) MRI of four CDKL5 patients in the first year of life. Compared with a healthy control (HC on the right), there is mild ventricular and CSF space enlargement more prominent in the frontal regions. Sagittal sequences demonstrate absence of cerebellar atrophy. (B–G) Progressive supratentorial and cerebellar atrophy in CDKL5. MRI performed in subject 7 at 4 (B–D) and 13 (E–G) years of life. There is evidence of progressive enlargement of supratentorial ventricles and CSF spaces (B, E) and widening of the interfolial cerebellar spaces of both cerebellar hemispheres (C, F) and vermis (D, G). (H–M) MRI performed in subject 6 at 3 years of age demonstrates signal alterations in central tegmental tracts (H, arrow) associated with diffusion restriction (I–J) and signal alterations in dentate nuclei bilaterally (K, arrow). There is subtle widening of pericerebellar CSF spaces (L) and of supratentorial ventricle and CSF spaces, more prominent in frontal regions (M).

**Table 3.** Volume whole-brain vertex-wise between-group cluster analysis.

| LEFT HEMISPHERE |                  |       |       |       |                            | RIGHT HEMISPHERE |                  |      |       |       |                            |
|-----------------|------------------|-------|-------|-------|----------------------------|------------------|------------------|------|-------|-------|----------------------------|
| Area            | Z <sub>max</sub> | X     | Y     | Z     | Brain region               | Area             | Z <sub>max</sub> | X    | Y     | Z     | Brain region               |
| 1414.58         | -4.02            | -44.6 | 6.0   | -26.6 | Superior temporal          | 853.37           | -7.16            | 53.0 | 2.9   | -15.5 | Superior temporal          |
| 526.95          | -5.87            | -10.4 | -42.0 | -1.0  | Rostral anterior cingulate | 254.83           | -4.38            | 55.7 | -22.8 | -16.6 | Middle temporal            |
| 411.30          | -4.02            | -48.3 | -44.4 | -12.3 | Inferior temporal          | 138.09           | -3.84            | 31.8 | -47.9 | -2.4  | Lingual                    |
|                 |                  |       |       |       |                            | 381.09           | -3.56            | 11.8 | -43.1 | -2.1  | Rostral anterior cingulate |

Whole-brain statistical analysis of significant group differences in volumetric measurements, in the left and right hemispheres of patients with CDKL5 mutation and controls (CDKL5 > CTRL, false discovery rate (FDR) multiple correction with cluster wise  $p_{\text{value}}(\text{CWP}) < 0.05$ ). Area, surface area of the significant clusters (mm<sup>2</sup>); X, Y, Z, MNI coordinates of the peak (mm); brain region, region parceled according to [Desikan et al. \(2006\)](#) labels.

brain atrophy also appeared after the age of 20 months in a patient with previously normal brain MRI ([Sartori et al. 2011](#)).

Non-specific abnormalities have been reported less frequently, such as T2 fluid-attenuated inversion recovery hyperintensities in the white matter, hyperintensities in the dentate nuclei, and delayed myelination ([Archer et al. 2006](#); [Buoni et al. 2006](#); [Bahi-Buisson et al. 2008](#); [Elia et al. 2008](#); [Pintaudi et al. 2008](#); [Russo et al. 2009](#); [Stalpers et al. 2012](#)). Neither cortical malformations nor dysplasia have been observed ([Bahi-Buisson et al. 2008](#)).

In our cohort, we found corpus callosum thinning in 31.8% of patients, and symmetric T2-hyperintensity involving the central tegmental tracts (CTT) in 18.2%, the posterior periventricular white matter in 13.6%, and the dentate nuclei in 13.6% of patients. CTT is one of the earliest regions of myelination and its hyperintensities are an unusual and aetiologically unclear neuroimaging finding ([Nathan and Smith 1982](#)) already reported in children with different underlying conditions, including epilepsy, cerebral palsy, neoplasm, various neurodevelopmental, and metabolic

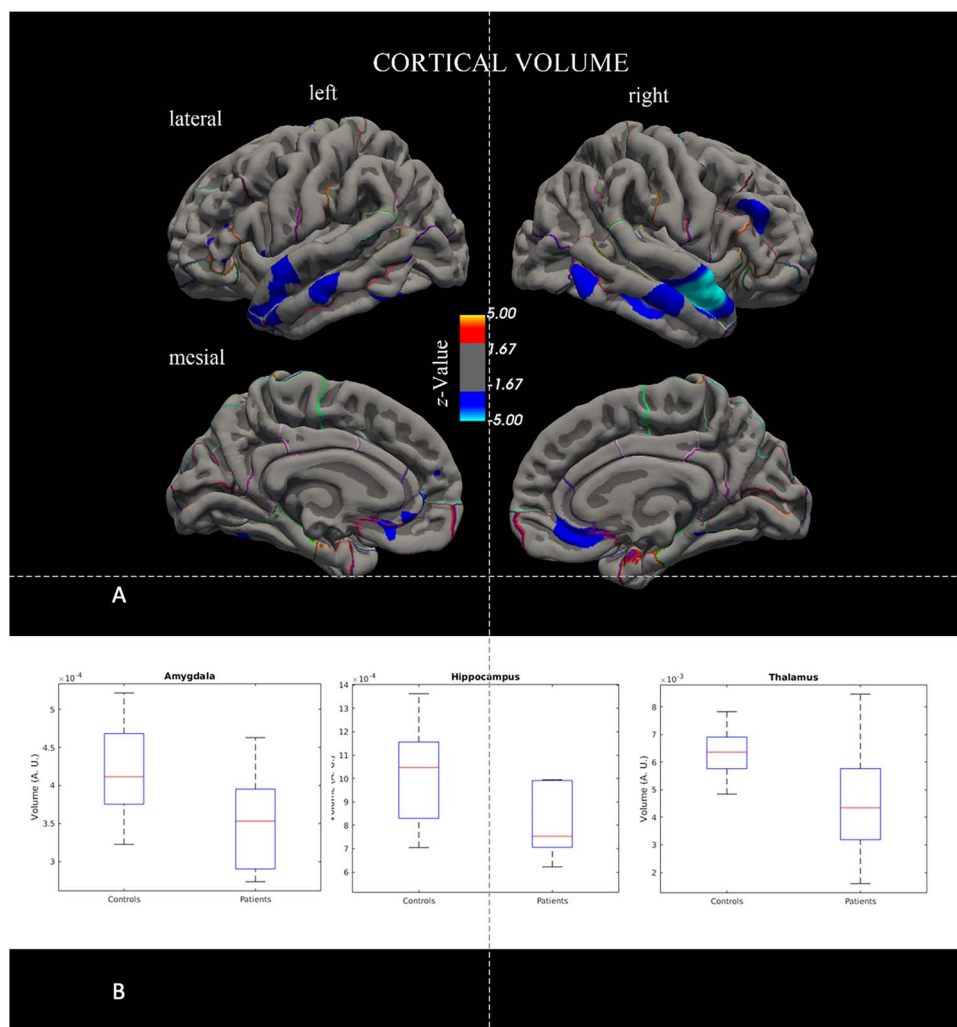


**Fig. 3.** (A) Statistical whole-brain group analysis of the cortical volume in CDKL5-related patients compared with healthy controls using the intracranial volume as covariate. Z-value maps are superimposed on the pial surfaces of the left and right hemispheres. (B) Plots showing the differences in hippocampus, thalamus, and amygdala between patients and controls. The P-values associated with them are reported in Table 2.

disorders (Takanashi et al. 2006; Yoshida et al. 2009; Singh et al. 2015). Neuropathological studies have suggested that CTT lesions seen at MRI may be due to gliosis, vacuolization, neuronal loss, demyelination, and necrosis (Shioda et al. 2011).

The most original findings of our study derive from the quantitative MRI analysis, where we found a volumetric reduction of the whole brain, including both the white and cortical gray matter, with a reduction of surface area (SA), mainly over the temporal regions, with a maximum in the superior temporal gyri, with no reduction in cortical thickness. Although SA is related to the number of cortical columns (Rakic and Swaab 1988), thickness (Vuoksimaa et al. 2015), rather reflects migration, and post-migrational organization. Global cognitive abilities seem to be primarily driven by the cortical SA (Huttenlocher 1990). Quantitative analysis of brain ROIs uncovered atrophic patterns in the frontal and temporal lobes, with more statistical significances in the clusters located in the superior and middle temporal regions, as assessed by the cluster-wise analysis.

Although quantitative neuroimaging in CDD patients have not been performed before, quantitative MRI analysis in other developmental and epileptic encephalopathies (DEEs) had already highlighted volumetric brain reduction. Patients with Dravet syndrome exhibit a reduction of total brain volume, including

gray and white matter, and a reduced surface area with some difference across cerebral regions (Lee et al. 2017). A similar finding has been described in PCDH19-related patients, with a prominent reduction of cortical gyrification in the temporal regions with a reduced cortical area and preserved cortical thickness (Lenge et al. 2020).

Neurobiologically, the reduction in cortical volume we observed in CDD might reflect reductions in dendritic arborization (Ren et al. 2019; Zhu and Xiong 2019) and spine density, PSD-95-positive synaptic puncta, and alterations in spine morphology (Della Sala et al. 2016; Lupori et al. 2019; Ren et al. 2019) described in CDKL5 KO mouse models (Chen et al. 2010). CDKL5 is localized at excitatory synapses and contributes to correct dendritic spine structure and synapse activity, binding and phosphorylating the cell adhesion molecule NGL-1 (Kim et al. 2006; Woo et al. 2009; Ricciardi et al. 2012). Silencing CDKL5 leads to a significant reduction of density and length of dendritic spines, both in vitro and in vivo (Ricciardi et al. 2012). The role of CDKL5 in spine development and synapse activity was also confirmed in iPSC-derived neurons from patients with CDD (Ricciardi et al. 2012). In the CDKL5 null brain, magnetic resonance spectroscopy (MRS) revealed metabolic dysregulation, which may resemble mitochondrial dysfunction (Carli et al. 2021).

Neuropathological studies on a 5-year-old boy with CDD who died of SUDEP, showed an abnormal configuration of bilateral superior temporal gyri, which appeared deeply buried, and an enlargement of lateral and third ventricles (Paine et al. 2012). This report may be consistent with the abnormal findings involving the temporal regions uncovered by our quantitative analysis. Neuropathological studies detected microscopically abnormalities of Purkinje cell layers (Paine et al. 2012), which could not be detected by our quantitative analysis. The involvement of cerebellum was also highlighted in a mouse model, where impaired GABAergic cerebellar transmission was demonstrated (Sivilia et al. 2016).

Our study has the following limitations: (i) brain MRI imaging was performed at seizure onset in all patients and additional MRI imaging were done at different ages, according to clinical indications; (ii) our retrospective analysis does not allow the association of brain MRI findings with measures of clinical severity and EEG features; (iii) MRI was assessed by visual inspection in most patients and quantitative or statistical techniques could only be performed in five; (iv) the study population consists of a subset of patients with CDD with severe refractory epilepsy, and no data are available for seizure-free patients: these patients will be included in following prospective studies.

CDD is not considered to be a neurodegenerative disorder, but our study suggests a progression of brain atrophy. Although the time-course of atrophy progression remains to be determined, it seems to be a common finding in early onset DEEs. Prospective quantitative brain MRI analyses in an expanded series are needed to draw conclusions on macroscopic neuroanatomy of CDD, including structural-clinical correlates. It would be particularly indicated to include this imaging analysis in prospective natural history studies on CDD, as MRI might represent an imaging biomarker for measuring the effects of emerging gene therapies on macroscopic brain structure.

## Acknowledgments

We would like to thank the patients and their families for participation in this study.

## CRedit author statement

Nicola Specchio (Conceptualization, Data curation, Formal analysis, Methodology, Writing—original draft, Writing—review and editing), Marina Trivisano (Conceptualization, Data curation, Writing—original draft), Matteo Lenge (Conceptualization, Data curation, Formal analysis, Methodology, Validation, Writing—review and editing), Alessandro Ferretti (Data curation, Methodology), Davide Mei (Data curation, Formal analysis, Writing—review and editing), Elena Parrini (Validation, Writing—review and editing), Antonio Napolitano (Methodology, Validation, Writing—review and editing), Maria Camilla Rossi Espagnet (Data curation, Formal analysis, Writing—review and editing), Giacomo Talenti (Data curation, Formal analysis, Writing—original draft), Daniela Longo (Data curation, Formal analysis, Writing—review and editing), Jacopo Proietti (Data curation, Formal analysis, Investigation, Writing—review and editing), Francesca Ragona (Data curation, Formal analysis, Writing—review and editing), Elena Freri (Data curation, Formal analysis, Writing—review and editing), Roberta Solazzi (Data curation, Formal analysis, Writing—review and editing), Tiziana Granata (Data curation, Formal analysis, Writing—review and editing), Francesca Darra (Data curation, Formal analysis, Writing—review and editing), Bernardo Dalla Bernardina (Conceptualization, Supervision, Writing—review

and editing), Federico Vigeveno (Conceptualization, Supervision, Writing—review and editing), Renzo Guerrini (Conceptualization, Data curation, Formal analysis, Supervision, Validation, Writing—review and editing).

## Supplementary material

Supplementary material is available at *Cerebral Cortex* online.

## Funding

R.G., M.L., D.M., and E.P. were supported by Tuscany Region Call for Health 2018 (grant DECODE-EE), and the Brain Optical Imaging Project by the Fondazione Cassa di Risparmio di Firenze.

*Conflict of interest statement:* Authors report no conflict of interest for this paper.

## Disclosure

We confirm that we have read the Journal's position on issues involved in ethical publication and affirm that this report is consistent with those guidelines.

## References

- Archer HL, Evans J, Edwards S, Colley J, Newbury-Ecob R, O'Callaghan F, Huyton M, O'Regan M, Tolmie J, Sampson J, et al. CDKL5 mutations cause infantile spasms, early onset seizures, and severe mental retardation in female patients. *J Med Genet.* 2006;43:729–734.
- Arican P, Gencpinar P, Olgac DN. A new cause of developmental and epileptic encephalopathy with continuous spike-and-wave during sleep: CDKL5 disorder. *Neurocase.* 2019;25:59–61.
- Bahi-Buisson N, Kaminska A, Boddaert N, Rio M, Afenjar A, Gérard M, Giuliano F, Motte J, Héron D, Morel MANG, et al. The three stages of epilepsy in patients with CDKL5 mutations. *Epilepsia.* 2008;49:1027–1037.
- Bahi-Buisson N, Nectoux J, Rosas-Vargas H, Milh M, Boddaert N, Girard B, Cances C, Ville D, Afenjar A, Rio M, et al. Key clinical features to identify girls with CDKL5 mutations. *Brain.* 2008;131:2647–2661.
- Bahi-Buisson N, Villeneuve N, Caietta E, Jacqueline A, Maurey H, Matthijs G, Van Esch H, Delahaye A, Moncla A, Milh M, et al. Recurrent mutations in the CDKL5 gene: genotype-phenotype relationships. *Am J Med Genet A.* 2012;158A:1612–1619.
- Buoni S, Zannolli R, Colamaria V, Macucci F, di Bartolo RM, Corbini L, Orsi A, Zappella M, Hayek J. Myoclonic encephalopathy in the CDKL5 gene mutation. *Clin Neurophysiol.* 2006;117:223–227.
- Carli S, Chaabane L, Butti C, De Palma C, Aïmar P, Salio C, Vignoli A, Giustetto M, Landsberger N, Frasca A. In vivo magnetic resonance spectroscopy in the brain of Cdk5 null mice reveals a metabolic profile indicative of mitochondrial dysfunctions. *J Neurochem.* 2021;157:1253–1269.
- Chen Q, Zhu Y-C, Yu J, Miao S, Zheng J, Xu L, Zhou Y, Li D, Zhang C, Tao J, et al. CDKL5, a protein associated with Rett syndrome, regulates neuronal morphogenesis via Rac1 signaling. *J Neurosci.* 2010;30:12777–12786.
- Darra F, Monchelato M, Loos M, Juanes M, Bernardina BD, Valenzuela GR, Gallo A, Caraballo R. CDKL5-associated developmental and epileptic encephalopathy: a long-term, longitudinal electroclinical study of 22 cases. *Epilepsy Res.* 2023;190:107098.

- Della Sala G, Putignano E, Chelini G, Melani R, Calcagno E, Michele Ratto G, Amendola E, Gross CT, Giustetto M, Pizzorusso T. Dendritic spine instability in a mouse model of CDKL5 disorder is rescued by insulin-like growth factor 1. *Biol Psychiatry*. 2016;80:302–311.
- Demarest S, Pestana-Knight EM, Olson HE, Downs J, Marsh ED, Kaufmann WE, Partridge C-A, Leonard H, Gwadry-Sridhar F, Frame KE, et al. Severity assessment in CDKL5 deficiency disorder. *Pediatr Neurol*. 2019;97:38–42.
- Desikan RS, Ségonne F, Fischl B, Quinn BT, Dickerson BC, Blacker D, Buckner RL, Dale AM, Maguire RP, Hyman BT, et al. An automated labeling system for subdividing the human cerebral cortex on MRI scans into gyral based regions of interest. *NeuroImage*. 2006;31:968–980.
- Elia M, Falco M, Ferri R, Spalletta A, Bottitta M, Calabrese G, Carotenuto M, Musumeci SA, Lo Giudice M, Fichera M. CDKL5 mutations in boys with severe encephalopathy and early-onset intractable epilepsy. *Neurology*. 2008;71:997–999.
- Fehr S, Wong K, Chin R, Williams S, de Klerk N, Forbes D, Krishnaraj R, Christodoulou J, Downs J, Leonard H. Seizure variables and their relationship to genotype and functional abilities in the CDKL5 disorder. *Neurology*. 2016;87:2206–2213.
- Garel C, Cont I, Alberti C, Jossereand E, Moutard ML, Ducou le Pointe H. Biometry of the corpus callosum in children: MR imaging reference data. *AJNR Am J Neuroradiol*. 2011;32:1436–1443.
- Guerrini R, Parrini E. Epilepsy in Rett syndrome, and CDKL5 - and FOXG1 -gene-related encephalopathies. *Epilepsia*. 2012;53:2067–2078.
- Guha Roy A, Conjeti S, Navab N, Wachinger C. QuickNAT: a fully convolutional network for quick and accurate segmentation of neuroanatomy. *NeuroImage*. 2019;186:713–727.
- Hagebeuk EEO, van den Bossche RAS, de Weerd AW. Respiratory and sleep disorders in female children with atypical Rett syndrome caused by mutations in the CDKL5 gene. *Dev Med Child Neurol*. 2013;55:480–484.
- Huttenlocher PR. Morphometric study of human cerebral cortex development. *Neuropsychologia*. 1990;28:517–527.
- Kadam SD, Sullivan BJ, Goyal A, Blue ME, Smith-Hicks C. Rett syndrome and CDKL5 deficiency disorder: from bench to clinic. *Int J Mol Sci*. 2019;20.
- Kim S, Burette A, Chung HS, Kwon S-K, Woo J, Lee HW, Kim K, Kim H, Weinberg RJ, Kim E. NGL family PSD-95–interacting adhesion molecules regulate excitatory synapse formation. *Nat Neurosci*. 2006;9:1294–1301.
- Lee Y-J, Yum M-S, Kim M-J, Shim W-H, Yoon HM, Yoo IH, Lee J, Lim BC, Kim KJ, Ko T-S. Large-scale structural alteration of brain in epileptic children with SCN1A mutation. *NeuroImage Clin*. 2017;15:594–600.
- Lenge M, Marini C, Canale E, Napolitano A, De Masi S, Trivisano M, Mei D, Longo D, Rossi Espagnet MC, Lucenteforte E, et al. Quantitative MRI-based analysis identifies developmental limbic abnormalities in PCDH19 encephalopathy. *Cereb Cortex*. 2020;30:6039–6050.
- Liang J-S, Shimojima K, Takayama R, Natsume J, Shichiji M, Hirasawa K, Imai K, Okanishi T, Mizuno S, Okumura A, et al. CDKL5 alterations lead to early epileptic encephalopathy in both genders. *Epilepsia*. 2011;52:1835–1842.
- Lo Martire V, Alvente S, Bastianini S, Berteotti C, Silvani A, Valli A, Viggiano R, Ciani E, Zoccoli G. CDKL5 deficiency entails sleep apneas in mice. *J Sleep Res*. 2017;26:495–497.
- Lupori L, Sagona G, Fuchs C, Mazziotti R, Stefanov A, Putignano E, Napoli D, Strettoi E, Ciani E, Pizzorusso T. Site-specific abnormalities in the visual system of a mouse model of CDKL5 deficiency disorder. *Hum Mol Genet*. 2019;28:2851–2861.
- Mangatt M, Wong K, Anderson B, Epstein A, Hodgetts S, Leonard H, Downs J. Prevalence and onset of comorbidities in the CDKL5 disorder differ from Rett syndrome. *Orphanet J Rare Dis*. 2016;11:39.
- Mei D, Marini C, Novara F, Bernardina BD, Granata T, Fontana E, Parrini E, Ferrari AR, Murgia A, Zuffardi O, et al. Xp22.3 genomic deletions involving the CDKL5 gene in girls with early onset epileptic encephalopathy. *Epilepsia*. 2010;51:647–654.
- Melani F, Mei D, Pisano T, Savasta S, Franzoni E, Ferrari AR, Marini C, Guerrini R. CDKL5 gene-related epileptic encephalopathy: electroclinical findings in the first year of life. *Dev Med Child Neurol*. 2011;53:354–360.
- Nathan PW, Smith MC. The rubrospinal and central tegmental tracts in man. *Brain*. 1982;105:223–269.
- Olson HE, Poduri A. CDKL5 mutations in early onset epilepsy: case report and review of the literature. *J Pediatr Epilepsy*. 2012;1:151–159.
- Olson HE, Demarest ST, Pestana-Knight EM, Swanson LC, Iqbal S, Lal D, Leonard H, Cross JH, Devinsky O, Benke TA. Cyclin-dependent kinase-like 5 deficiency disorder: clinical review. *Pediatr Neurol*. 2019;97:18–25.
- Paine SML, Munot P, Carmichael J, Das K, Weber MA, Prabhakar P, Jacques TS. The neuropathological consequences of CDKL5 mutation. *Neuropathol Appl Neurobiol*. 2012;38:744–747.
- Pintaudi M, Baglietto MG, Gaggero R, Parodi E, Pessagno A, Marchi M, Russo S, Veneselli E. Clinical and electroencephalographic features in patients with CDKL5 mutations: two new Italian cases and review of the literature. *Epilepsy Behav*. 2008;12:326–331.
- Rakic P, Swaab DF. Defects of neuronal migration and the pathogenesis of cortical malformations. *Prog Brain Res*; 1988;73:15–37.
- Ren E, Roncacé V, Trazzi S, Fuchs C, Medici G, Gennaccaro L, Loi M, Galvani G, Ye K, Rimondini R, et al. Functional and structural impairments in the perirhinal cortex of a mouse model of CDKL5 deficiency disorder are rescued by a TrkB agonist. *Front Cell Neurosci*. 2019;13:169.
- Ricciardi S, Ungaro F, Hambrock M, Rademacher N, Stefanelli G, Brambilla D, Sessa A, Magagnotti C, Bachi A, Giarda E, et al. CDKL5 ensures excitatory synapse stability by reinforcing NGL-1-PSD95 interaction in the postsynaptic compartment and is impaired in patient iPSC-derived neurons. *Nat Cell Biol*. 2012;14:911–923.
- Rusconi L, Salvatoni L, Giudici L, Bertani I, Kilstrop-Nielsen C, Broccoli V, Landsberger N. CDKL5 expression is modulated during neuronal development and its subcellular distribution is tightly regulated by the C-terminal tail. *J Biol Chem*. 2008;283:30101–30111.
- Russo S, Marchi M, Cogliati F, Bonati MT, Pintaudi M, Veneselli E, Saletti V, Balestrini M, Ben-Zeev B, Larizza L. Novel mutations in the CDKL5 gene, predicted effects and associated phenotypes. *Neurogenetics*. 2009;10:241–250.
- Sartori S, Polli R, Bettella E, Rossato S, Andreoli W, Vecchi M, Giordano L, Accorsi P, Di Rosa G, Toldo I, et al. Pathogenic role of the X-linked cyclin-dependent kinase-like 5 and aristaless-related homeobox genes in epileptic encephalopathy of unknown etiology with onset in the first year of life. *J Child Neurol*. 2011;26:683–691.
- Shioda M, Hayashi M, Takanashi J, Ichi, Osawa M. Lesions in the central tegmental tract in autopsy cases of developmental brain disorders. *Brain Dev*. 2011;33:541–547.

- Singh P, Kaur A, Kaur R, Aggarwal S, Singh R. Symmetrical central tegmental tract hyperintensities on magnetic resonance imaging. *J Pediatr Neurosci*. 2015;10:235–236.
- Sivilia S, Mangano C, Beggiato S, Giuliani A, Torricella R, Baldassarro VA, Fernandez M, Lorenzini L, Giardino L, Borelli AC, et al. CDKL5 knockout leads to altered inhibitory transmission in the cerebellum of adult mice. *Genes, Brain Behav*. 2016;15:491–502.
- Stalpers XL, Spruijt L, Yntema HG, Verrips A. Clinical phenotype of 5 females with a CDKL5 mutation. *J Child Neurol*. 2012;27:90–93.
- Takanashi JI, Kanazawa M, Kohno Y. Central tegmental tract involvement in an infant with 6-pyruvoyltetrahydropterin synthetase deficiency. *Am J Neuroradiol*. 2006;27:584–585.
- Tang Y, Wang ZI, Sarwar S, Choi JY, Wang S, Zhang X, Parikh S, Moosa AN, Pestana-Knight E. Brain morphological abnormalities in children with cyclin-dependent kinase-like 5 deficiency disorder. *Eur J Paediatr Neurol*. 2021;31:46–53.
- Vuoksima E, Panizzon MS, Chen C-H, Fiecas M, Eyler LT, Fennema-Notestine C, Hagler DJ, Fischl B, Franz CE, Jak A, et al. The genetic association between neocortical volume and general cognitive ability is driven by global surface area rather than thickness. *Cereb Cortex*. 2015;25:2127–2137.
- Weaving LS, Christodoulou J, Williamson SL, Friend KL, McKenzie OLD, Archer H, Evans J, Clarke A, Pelka GJ, Tam PPL, et al. Mutations of CDKL5 cause a severe neurodevelopmental disorder with infantile spasms and mental retardation. *Am J Hum Genet*. 2004;75:1079–1093.
- Woo J, Kwon S-K, Choi S, Kim S, Lee J-R, Dunah AW, Sheng M, Kim E. Trans-synaptic adhesion between NGL-3 and LAR regulates the formation of excitatory synapses. *Nat Neurosci*. 2009;12:428–437.
- Yoshida S, Hayakawa K, Yamamoto A, Aida N, Okano S, Matsushita H, Kanda T, Yamori Y, Yoshida N, Hirota H. Symmetrical central tegmental tract (CTT) hyperintense lesions on magnetic resonance imaging in children. *Eur Radiol*. 2009;19:462–469.
- Zhou A, Han S, Zhou ZJ. Molecular and genetic insights into an infantile epileptic encephalopathy – CDKL5 disorder. *Front Biol (Beijing)*. 2017;12(1):1–6.
- Zhou A, Xiong ZQ. Molecular and synaptic bases of CDKL5 disorder. *Dev Neurobiol*. 2019;79(1):8–19.
- Zhu YC, Li D, Wang L, Lu B, Zheng J, Zhao SL, Zeng R, Xiong ZQ. Palmitoylation-dependent CDKL5-PSD-95 interaction regulates synaptic targeting of CDKL5 and dendritic spine development. *Proc Natl Acad Sci USA*. 2013;110:9118–9123.
- Zuberi SM, Wirrell E, Yozawitz E, Wilmshurst JM, Specchio N, Riney K, Pressler R, Auvin S, Samia P, Hirsch E, et al. ILAE classification and definition of epilepsy syndromes with onset in neonates and infants: position statement by the ILAE task force on nosology and definitions. *Epilepsia*. 2022;63:1349–1397.